

## Electronic Supplementary Information

### One-pot *in situ* solvothermal synthesis of ZnCo<sub>2</sub>S<sub>4</sub>/carbon nanosphere composites: tuning carbon content for high-performance supercapacitor electrodes

Raji Yuvaraja <sup>a</sup>, Sankar Sarathkumar <sup>a</sup>, Venkatesan Gowsalya <sup>a</sup>, Sorna Pandian Anitha Juliet <sup>a</sup>, Selvakumar Veeralakshmi <sup>b</sup>, Siva Kalaiselvam <sup>b</sup>, Gunniya Hariyanandam Gunasekar <sup>c,d</sup> and Selvan Nehru<sup>\*a</sup>

<sup>a</sup>Department of Physical Chemistry, University of Madras, Guindy Campus, Chennai, Tamil Nadu, India, 600 025.

<sup>b</sup>Centre for Industrial Safety, Anna University, Chennai - 600025, Tamil Nadu, India.

<sup>c</sup>Department of Catalysis and Fine Chemicals, CSIR-Indian Institute of Chemical Technology, Hyderabad-500007, India.

<sup>d</sup>CSIR-Academy of Scientific and Innovative Research (CSIR-AcSIR), Ghaziabad-201002, India.

\* Corresponding author's e-mail: nehruchem@gmail.com

#### 1. Materials and methods

All chemicals used in this study were of analytical grade and used as received without further purification. Zinc acetate dihydrate, cobalt acetate tetrahydrate, thioacetamide, dextrose, sodium lauryl sulfate (SLS), potassium hydroxide (KOH), ethylene glycol (EG) and N-methyl pyrrolidine (NMP) were purchased from Sisco Research Laboratories Pvt. Ltd. Acetylene black and polyvinylidene fluoride (PVDF) were purchased from Sigma-Aldrich. Polyvinyl alcohol (PVA, Mw = ~1,15,000) was obtained from Loba Chemie Pvt. Ltd. Deionized (DI) water was used throughout the studies. Before use, the nickel plate (99% purity, thickness: 0.5 mm), stainless-steel sheets (SS-304, thickness: 0.1 mm) were polished with P220 emery paper for surface activation, then sequentially cleaned in 1 M HCl for 15 minutes and acetone for 30 minutes using ultrasonication to remove any surface residues.

***In situ* solvothermal carbonization of ZnCo<sub>2</sub>O<sub>4</sub>/CNS (D2) nanocomposites.** For the comparison with ZnCo<sub>2</sub>S<sub>4</sub>/CNS (D2), the analogous ZnCo<sub>2</sub>O<sub>4</sub>/CNS (D2) was synthesized via *in situ* solvothermal carbonization without using thioacetamide as sulfur source as follows:<sup>1</sup> Zn(CH<sub>3</sub>COO)<sub>2</sub>·2H<sub>2</sub>O (0.44 g, 2 mmol) and Co(CH<sub>3</sub>COO)<sub>2</sub>·2H<sub>2</sub>O (0.97 g, 4 mmol) were dissolved in 40 mL of EG. Furthermore, urea (0.6 g, 10 mmol) and hexamine (1.4 g, 10 mmol), serve as alkali sources and shape-controlling agents, dextrose (0.36 g, 2.0 mmol) and SLS (0.58 g, 2.0 mmol), serving as the carbon source and surfactant, respectively and added gradually to the reaction solution, ensuring continuous stirring for 30 min. Further, the obtained pink color mixture was transported into a 100 mL Teflon-lined stainless-steel autoclave, and heated in a muffle furnace at 180 °C for 12 h. Finally, the resultant black precipitate was filtered after cooling to room temperature, washed three times with deionized water and ethanol, and then dried at 60 °C for 5 h. (Black solid, yield: 0.53 g).

## 2. Materials characterization

X-ray diffraction (XRD) patterns of samples were obtained using a Bruker D8 Advance X-ray diffractometer with Cu-K $\alpha$  radiation in the 2 $\theta$  range of 10°–80°. Raman spectra of samples were collected from a Horiba Raman spectrometer using a 532 nm laser source. Fourier transform infrared (FT-IR) spectroscopy was performed on Bruker mid-IR spectrometer. Surface morphology of the samples were examined by a CARL ZEISS GEMINI 500 field emission scanning electron microscopy (FESEM). BET surface area and BJH pore size distribution of samples were obtained from the N<sub>2</sub> adsorption-desorption isotherm technique using a BELSORP II (BEL Japan Inc.) instrument. X-ray photoelectron spectroscopy (XPS) was carried out on a PHI 5000 Versa Probe III photoelectron spectrometer (ULVAC-PHI, Inc., Japan) equipped with a monochromatic Al K $\alpha$  source ( $\lambda = 1486.7$  eV). All electrochemical measurements were carried out using the K-Lyte 1.3 (PG-Lyte) electrochemical workstation (Kanopy Techno Solutions, India). Electrochemical impedance spectroscopy (EIS) measurements were performed using the CHI660E workstation in the frequency range of 0.1 Hz to 100 kHz with a potential amplitude of 10 mV. A wettability test was conducted on Drop Master, DMe-211 plus.

## 3. Three-electrode SC studies

For the three-electrode SC studies, aqueous 3 M KOH solution as the electrolyte, Hg/HgO electrode as the reference electrode and platinum wire as the counter electrode were used. The working electrode was prepared by slurring the nanomaterial (80 wt%), acetylene black (10 wt%) as conducting material, and PVDF (10 wt%) as binder NMP as solvent. Then the resultant slurry was coated on the surface of the nickel plate current collector (1.5 cm x 1.5 cm), followed by drying at 60 °C for 5 h. The mass loading of active materials on the nickel plate was calculated by weighing the plate before and after the loading of active material. Cyclic voltammetry (CV) experiments were performed in the potential range of 0 to 0.6 V at various scan rates (10, 20, 40, 60, 80 and 100 mV s<sup>-1</sup>). Galvanostatic charge–discharge (GCD) studies were performed in the potential window of 0 to 0.5 V at different current densities (1, 2, 3, 4, 5, 10 and 15 A g<sup>-1</sup>). The specific capacitance ( $C_s$ ) and specific capacity ( $Q$ ) of the electrode were calculated from the GCD curves using the equation (S1 and S2).<sup>2</sup>

$$C_s = \frac{I \times \Delta t}{m \times \Delta V} \quad (S1)$$

$$Q = \frac{C_s \times \Delta V}{3.6} \quad (S2)$$

where  $C_s$  (F g<sup>-1</sup>),  $Q$  (mAh g<sup>-1</sup>),  $I$  (A),  $\Delta t$  (s),  $\Delta V$  (V) and  $m$  (g) represent the specific capacitance, specific capacity, constant discharge current, time taken for discharging, potential drop upon discharging and mass loading of the active material on the electrode, respectively.

#### 4. Two-electrode symmetric and asymmetric SC studies

For the two-electrode SC studies, the symmetric SCs were fabricated using a Swagelok type cell by sandwiching the two symmetric electrodes using the Whatman filter paper as separator and 3 M KOH as electrolyte. The symmetric electrodes were prepared by coating the slurry of active material consisting of  $\text{ZnCo}_2\text{S}_4/\text{CNS}$  (D2) (80 wt%), acetylene black (10 wt%) and PVDF (10 wt%) as a binder and NMP as a solvent on the two stainless steel (SS) plates (diameter: 1.7 cm and active area:  $2.27 \text{ cm}^2$ ). followed by drying thoroughly at  $60^\circ\text{C}$  for 5 h. By following the same method, the asymmetric two-electrode SC setup was constructed except one of the electrodes consists of active material as acetylene black (90 wt%) and PVDF (10 wt%).

Based on the GCD curves, the performance of the two-electrode SCs was evaluated by using equations (S3–S5) for symmetric and equations (S6–S8) for asymmetric configurations.<sup>2-4</sup>

For symmetric configurations,

$$Cs = 2 \times \frac{I \times \Delta t}{m \times \Delta V} \quad (\text{S3})$$

$$E = \frac{Cs \times (\Delta V)^2}{8 \times 3.6} \quad (\text{S4})$$

$$P = \frac{E}{\Delta t} \times 3600 \quad (\text{S5})$$

For asymmetric configurations,

$$Cs = \frac{I \times \Delta t}{m' \times \Delta V} \quad (\text{S6})$$

$$E = \frac{Cs \times (\Delta V)^2}{2 \times 3.6} \quad (\text{S7})$$

$$P = \frac{E}{\Delta t} \times 3600 \quad (\text{S8})$$

where E is the energy density ( $\text{W h kg}^{-1}$ ), P is the power density ( $\text{W kg}^{-1}$ ), m is the mass loading of the active material in one electrode for symmetric type (g), and m' is the total mass loading of the active materials in the anode and cathode electrodes for asymmetric type (g).

#### 5. Fabrication of all-solid-state asymmetric SC

To fabricate an all-solid-state SC, initially, the gel electrolyte was prepared as follows:<sup>3</sup> 3 g of PVA powder in 30 mL of DI water was heated to  $80^\circ\text{C}$  with constant stirring until the solution became clear. Then, aqueous KOH (1.5 g, 20 mL) was vigorously added to the above solution at  $80^\circ\text{C}$  until a clear solution was obtained. For the fabrication of asymmetric SC devices, the electrodes were prepared by coating the slurry of active material consisting of  $\text{ZnCo}_2\text{S}_4/\text{CNS}$  (D2) (80 wt%), acetylene black (10 wt%), PVDF (10 wt%) and using NMP on the three Ni plates (4.0 cm x 1.0 cm), and three electrodes consist of the active material as acetylene black (90 wt%) and

PVDF (10 wt%) using NMP on the three Ni plates and followed by drying thoroughly at 60 °C for 5 h. Then, the electrodes were immersed in the PVA-KOH gel solution for 5 min, followed by taking them out and allowing for solidification at room temperature. By following the hard pressing of two electrodes, a three-set of asymmetric SC devices was made and tested for open-circuit potential (OCP) measurement. Then three sets of asymmetric SC devices were connected in series and activated by the cyclic voltammetry method for 10 cycles. After charging, the device was tested to lighten the LED to evaluate the performance of the SC for real-time applications.

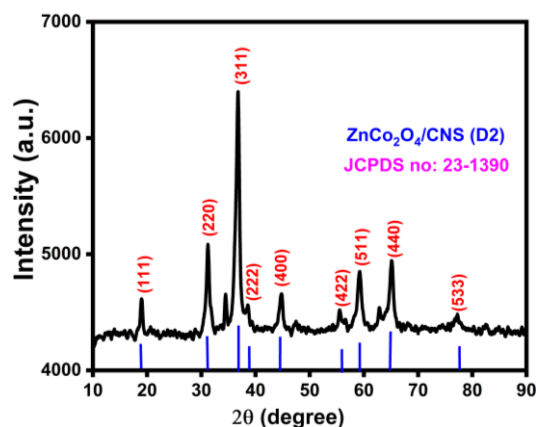


**Fig. S1** XRD pattern of  $\text{ZnCo}_2\text{O}_4/\text{CNS}$  (D2) sample.

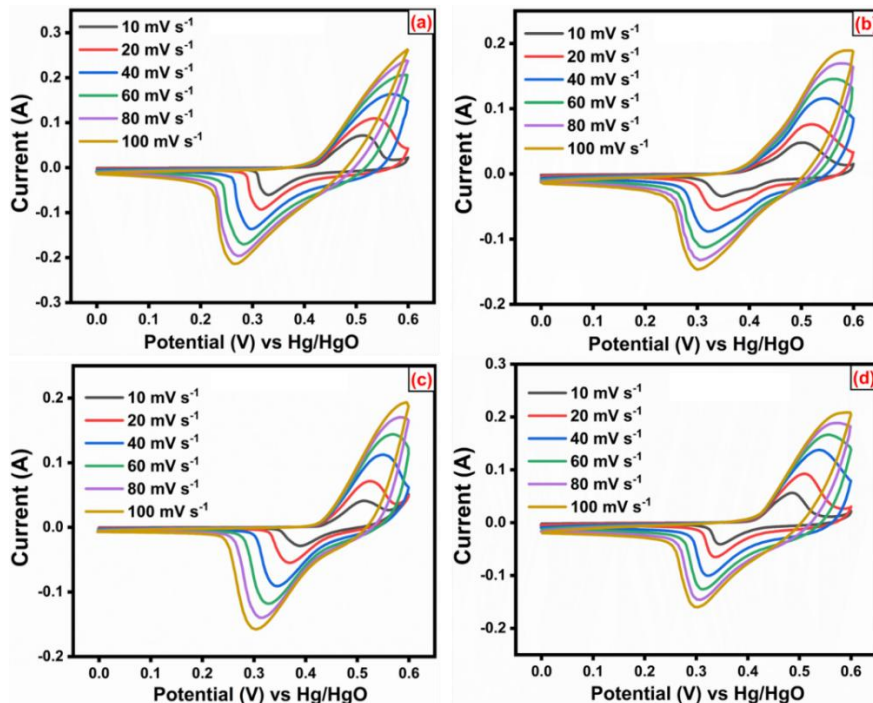


**Fig. S2** CV curves at different scan rates (10–100  $\text{mV s}^{-1}$ ): (a)  $\text{ZnCo}_2\text{S}_4/\text{CNS}$  (D1), (b)  $\text{ZnCo}_2\text{S}_4/\text{CNS}$  (D5), (c)  $\text{ZnCo}_2\text{S}_4/\text{CNS}$  (D10) and (d)  $\text{ZnCo}_2\text{O}_4/\text{CNS}$  (D2).

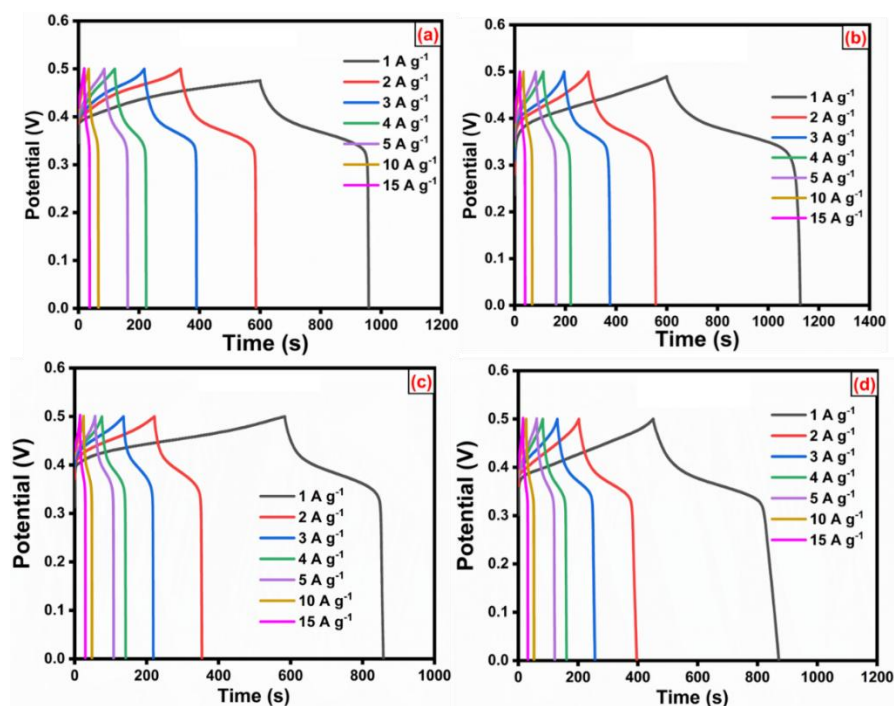


**Fig. S3** GCD curves at different current densities (1–15 A g<sup>-1</sup>): (a) ZnCo<sub>2</sub>S<sub>4</sub> (D1), (b) ZnCo<sub>2</sub>S<sub>4</sub> (D5), (c) ZnCo<sub>2</sub>S<sub>4</sub> (D10) and (d) ZnCo<sub>2</sub>O<sub>4</sub>/CNS (D2).

**Table S1** The calculated average crystallite size (nm) of ZnCo<sub>2</sub>S<sub>4</sub>, ZnCo<sub>2</sub>S<sub>4</sub>/CNS (Dx)-based composites using the Scherrer equation.

S. No	Sample	Average crystallite size (nm)
1	ZnCo <sub>2</sub> S <sub>4</sub>	18
2	ZnCo <sub>2</sub> S <sub>4</sub> /CNS (D1)	24
3	ZnCo <sub>2</sub> S <sub>4</sub> /CNS (D2)	42
4	ZnCo <sub>2</sub> S <sub>4</sub> /CNS (D5)	48
5	ZnCo <sub>2</sub> S <sub>4</sub> /CNS (D10)	55

**Table S2** Three-electrode specific capacitance and specific capacity of ZnCo<sub>2</sub>S<sub>4</sub>, ZnCo<sub>2</sub>O<sub>4</sub>/CNS (D2), CNS, and ZnCo<sub>2</sub>S<sub>4</sub>/CNS (Dx) based nanocomposites at current density 1 A g<sup>-1</sup> using 3 M KOH electrolyte.

S. No.	Electrode Materials	Specific capacitance (F g <sup>-1</sup> )	Specific capacity (mAh g <sup>-1</sup> )
1	ZnCo <sub>2</sub> S <sub>4</sub>	768	128
2	CNS	75	13
3	ZnCo <sub>2</sub> S <sub>4</sub> /CNS (D1)	716	119
<b>4</b>	<b>ZnCo<sub>2</sub>S<sub>4</sub>/CNS (D2)</b>	<b>1462</b>	<b>244</b>
5	ZnCo <sub>2</sub> S <sub>4</sub> /CNS (D5)	1164	194
6	ZnCo <sub>2</sub> S <sub>4</sub> /CNS (D10)	546	91
7	ZnCo <sub>2</sub> O <sub>4</sub> /CNS (D2)	730	122

**Table S3** Electrical parameters of ZnCo<sub>2</sub>S<sub>4</sub>, CNS, and ZnCo<sub>2</sub>S<sub>4</sub>/CNS (D2) electrode materials estimated using ZSimpWin circuit fitting software for EIS experimental data.

Electrode materials	$R_s$ ( $\Omega \text{ cm}^2$ )	$R_{\text{pore}}$ ( $\text{m}\Omega \text{ cm}^2$ )	$R_{\text{CT}}$ ( $\Omega \text{ cm}^2$ )	$Q_c$ ( $\text{mS cm}^{-2} \text{ s}^n$ )	$n$	$Q_{\text{dl}}$ ( $\mu\text{S cm}^{-2} \text{ s}^n$ )	$n$	$W$ ( $\mu\text{S cm}^{-2} \text{ s}^{0.5}$ )	$\chi^2$
ZnCo <sub>2</sub> S <sub>4</sub>	0.41	22.9	11.1	5.4	0.92	98.2	0.89	36.2	0.0032
CNS	1.07	57.7	$56.2 \times 10^{-6}$	1.2	0.70	480	0.90	103.4	0.0007
ZnCo <sub>2</sub> S <sub>4</sub> /CNS (D2)	0.56	30.3	9.4	4.9	0.89	21.9	1.00	21.0	0.0210

$R_s$  - solution resistance,  $R_{\text{pore}}$  - coating pore resistance,  $R_{\text{ct}}$  - charge transfer resistance,  $Q_c$  – coating capacitance,  $Q_{\text{dl}}$  – double-layer capacitance, CPE - constant phase element,  $n$  - exponent of CPE,  $W$  -Warburg impedance and  $\chi^2$  - chi-square value.

**Table S4** Comparison of the present work with previously reported ZnCo<sub>2</sub>S<sub>4</sub>-based nanocomposites.

S. No	Material	Method	Specific capacitance ( $\text{F g}^{-1}/^{\circ}\text{C g}^{-1}$ )	Capacity retention at no. of cycles	Ref.
1.	ZnCoS nanoparticles	Hydrothermal method	1269.1	91.6% at 5000 cycles	5
2.	ZnCoS-rGO hollow microsphere flower	Two-step hydrothermal method	1225.1	93.2% at 5000 cycles	6
3.	ZnCoS nanomaterial	Chemical precipitation and ion-exchange method	1134.1	81% at 6000 cycles	7
4.	Zn <sub>0.76</sub> Co <sub>0.24</sub> S	Facile oil phase approach	578	86.4% at 2000 cycles	8
5.	Zn-Co-S nanosheet array (NSA)/ Ni foam	Hydrothermal ion-exchange method	1904	78% at 5000 cycles	9
6.	Multilayer dodecahedron Zn-Co-S	Hydrothermal method	971.01	90.3% at 10000 cycles	10
7.	Co/Zn-S sandwiched graphene film	<i>In situ</i> method	1040	90.3% at 8000 cycles	11
8.	Mesoporous hollow ZnCo <sub>2</sub> S <sub>4</sub>	Solvothermal method	1045.3	95.5% at 5000 cycles	12
9.	MXene-wrapped ZnCo <sub>2</sub> S <sub>4</sub>	Two step hydrothermal method	1072	87.4% at 5000 cycles	13
10.	ZnCo <sub>2</sub> S <sub>4</sub> /CNS nanocomposite	<i>In situ</i> solvothermal method	1462	75% at 5000 cycles	<i>This report</i>

## References

1. L. Wu, L. Sun, X. Li, Q. Zhang, H. Si, Y. Zhang, K. Wang and Y. Zhang, *Appl. Surf. Sci.*, 2020, **506**, 144964.
2. R. Yuvaraja, S. Sarathkumar, V. Gowsalya, S. P. Anitha Juliet, S. Veeralakshmi, S. Kalaiselvam, S. Hussain and S. Nehru, *New J. Chem.*, 2024, **48**, 15556-15566.
3. R. Yuvaraja, S. Sarathkumar, V. Gowsalya, S. P. Anitha Juliet, S. Veeralakshmi, S. Kalaiselvam, G. H. Gunasekar and S. Nehru, *Energy Adv.*, 2024, DOI: 10.1039/D4YA00438H.
4. Y. Zhou, C. Li, X. Li, P. Huo and H. Wang, *Dalton Trans.*, 2021, **50**, 1097-1105.
5. H. Li, Z. Li, M. Sun, Z. Wu, W. Shen and Y. Q. Fu, *Electrochim. Acta*, 2019, **319**, 716-726.
6. P. Chen, C. Yang, P. Gao, X. Chen, Y.-J. Cheng, J. Liu and K. Guo, *Chem. Mater.*, 2022, **34**, 5896-5911.
7. Y. Zhang, N. Cao, S. Szunerits, A. Addad, P. Roussel and R. Boukherroub, *Chem. Eng. J.*, 2019, **374**, 347-358.
8. J. Yang, Y. Zhang, C. Sun, G. Guo, W. Sun, W. Huang, Q. Yan and X. Dong, *J. Mater. Chem. A*, 2015, **3**, 11462-11470.
9. J. Li, K. Chen, Y. Wang, W. Zhao, J. Zhou and L. Han, *ACS Appl. Energy Mater.*, 2021, **4**, 13803-13810.
10. J. Zhao, S. Hou, Y. Bai, Y. Lian, Q. Zhou, C. Ban, Z. Wang and H. Zhang, *Electrochim. Acta*, 2020, **354**, 136714.
11. N. Xin, Y. Liu, H. Niu, H. Bai and W. Shi, *J. Power Sources*, 2020, **451**, 227772.
12. C. Cheng, X. Zhang, C. Wei, Y. Liu, C. Cui, Q. Zhang and D. Zhang, *Ceram. Int.*, 2018, **44**, 17464-17472.
13. J.-Q. Qi, C.-C. Zhang, H. Liu, L. Zhu, Y.-W. Sui, X.-J. Feng, W.-Q. Wei, H. Zhang and P. Cao, *Rare Metals*, 2022, **41**, 2633-2644.